

# Improved pion mean fields and masses of singly heavy baryons

June-Young Kim<sup>1,2,\*</sup> and Hyun-Chul Kim<sup>2,3,†</sup>

<sup>1</sup>*Ruhr-Universität Bochum, Fakultät für Physik und Astronomie,  
Institut für Theoretische Physik II, D-44780 Bochum, Germany*

<sup>2</sup>*Department of Physics, Inha University, Incheon 22212, Republic of Korea*

<sup>3</sup>*School of Physics, Korea Institute for Advanced Study (KIAS), Seoul 02455, Republic of Korea*

(Dated: December 1, 2021)

A singly heavy baryon can be viewed as  $N_c - 1$  ( $N_c$  as the number of colors) light valence quarks bound by the pion mean fields that are created by the presence of the  $N_c - 1$  valence quarks self-consistently, while the heavy quark inside a singly heavy baryon is regarded as a static color source. We investigate how the pion mean fields are created by the presence of  $N_c$ ,  $N_c - 1$ , and  $N_c - 2$  light valence quarks, which correspond to the systems of light baryons, singly heavy baryons, and doubly heavy baryons. As the number of color decreases from  $N_c$  to  $N_c - 1$ , the pion mean fields undergo changes. As a result, the valence-quark contributions to the moments of inertia of the soliton become larger than the case of the  $N_c$  valence quarks, whereas the sea-quark contributions decrease systematically. On the other hand, the presence of the  $N_c - 2$  valence quarks is not enough to produce the strong pion mean fields, which leads to the fact that the classical soliton can not be formed. It indicates that the pion mean-field approach is not suitable to describe doubly heavy baryons. We show that the mass spectra of the singly heavy baryons are better described by the improved pion mean fields, compared with the previous work in which the pion mean fields are assumed to be intact with  $N_c$  varied.

Keywords: Masses of singly heavy baryons, improved pion mean fields, the chiral quark-soliton model

arXiv:1909.00123v2 [hep-ph] 2 Mar 2020

---

\* E-mail: Jun-Young.Kim@ruhr-uni-bochum.de

† E-mail: hchkim@inha.ac.kr

## I. INTRODUCTION

A light baryon can be regarded as a state of  $N_c$  (the number of colors) valence quarks bound by meson mean fields in the large  $N_c$  quantum chromodynamics (QCD) [1–3]. Since the nucleon mass is proportional to  $N_c$  whereas meson-loop fluctuations are suppressed by  $1/N_c$ , the mean-field approach is justified in the large  $N_c$  limit. The chiral quark-soliton model ( $\chi$ QSM) realizes effectively this idea of the pion mean-field approach [4–7]. The model has been very successful in describing the lowest-lying SU(3) light baryons. The same idea can be applied to a singly heavy baryon, which consists of two light valence quarks and one heavy quark. We can consider the heavy baryon as the  $N_c - 1$  light valence quarks bound by the pion mean fields [8]. In the limit of infinitely heavy quark mass ( $m_Q \rightarrow \infty$ ), the heavy quark can be regarded as a static color source. This pion mean-field approach has a great virtue because it describes both the light and singly heavy baryons on an equal footing. Recently, it was shown that the pion mean-field approach indeed describes very well the masses of the singly heavy baryons [9, 10]. The magnetic moments and electromagnetic form factors of the singly heavy baryons were also studied within this approach with all the parameters fixed in the light baryon sector [11, 12]. Very recently, the LHCb Collaboration announced the five or six excited  $\Omega_c$ 's, among which two of them have unusually small widths [13]. The Belle Collaboration confirmed the existence of the four excited  $\Omega_c$ 's [14]. In the  $\chi$ QSM, the two of the newly found excited  $\Omega_c$ 's were classified as the members of the baryon antidecaplet where remaining  $\Omega_c$ 's belong to the excited sextet representations [15]. The small widths of those two  $\Omega_c$ 's were well explained in the  $\chi$ QSM [16].

One can ask a critical question about the large  $N_c$  limit, since  $N_c$  and  $N_c - 1$  are parametrically not different when the limit of  $N_c \rightarrow \infty$  is taken. In fact, the large  $N_c$  limit is introduced to justify the mean-field approach in which the  $1/N_c$ -order meson fluctuations or in a more traditional language, particle-hole excitations, can be neglected. When it comes to the real world, i.e., when one sets  $N_c = 3$ , certain important physics of baryons attributed to the large  $N_c$  limit is still inherited. For example, the pion mean-field approach at  $N_c = 3$  describes very well various properties and observables of the lowest-lying SU(3) baryons (see for example a review [5]). The same is true if one takes  $N_c - 1 = 2$  as mentioned above. While  $N_c$  and  $N_c - 1$  are parametrically the same in the large  $N_c$  limit, the real world at  $N_c = 3$  exhibits certain difference between the light and singly heavy baryons. For example, the  $N_c = 3$  chiral soliton consists of three quarks such that the soliton is fermionic, whereas the  $N_c - 1 = 2$  soliton emerges as a colored bosonic soliton in the antisymmetric color state. It yields a singly-heavy baryon in the color singlet state when it is coupled to a heavy quark. Moreover, the hypercharge  $Y' = (N_c - 1)/3 = 2/3$  describes very well the SU(3) representations of the singly heavy baryons including excited ones (see for example, a recent review [17]). Thus, we will consider the large  $N_c$  limit in this work to justify the existence of the pion mean-field solution rather than a mathematically rigorous limit.

Previous works [9, 15, 16] employed an “model-independent approach”, which means that all the dynamical parameters were fixed by using the experimental data. While this approach has a merit to predict the experimental data without any model calculations, one can not decompose the valence- and sea-quark contributions, so that the overall replacement of the  $N_c$  factor by  $N_c - 1$  underestimates the sea-quark contributions. Thus, it is inevitable to introduce an additional parameter to compensate it. On the other hand, the self-consistent  $\chi$ QSM, where the pion mean fields are created explicitly by solving the classical equation of motion, assumed that the pion mean fields are not modified by changing the number of the valence quarks [12]. In Ref. [12], the number of the valence quarks  $N_c$  are merely replaced by  $N_c - 1$  to describe the singly heavy baryons with the same pion mean-field solutions used. However, we find that the number of the valence quarks indeed alter the pion mean fields, which will be shown in the present work. We expect that the reduction of the number of the valence quarks from  $N_c$  to  $N_c - 1$  will create weaker vacuum polarizations and as a result will lead to the weaker pion mean fields. In this work, we will explicitly compute the classical equations of motion to derive the pion mean-field solution, changing the number of the valence quarks. Interestingly, we find that the pion mean-field solutions do not exist when the number of the valence quarks is  $N_c - 2$ . This is understandable, since  $N_c - 2$  means practically a single light valence quark. The presence of a single valence quark is not enough to create a strong pion mean fields to bind a doubly heavy baryon. Thus, in any pion mean-field approaches, we are not able to describe a system of doubly heavy baryons. In the present work, we will revisit the mass splittings of the singly heavy baryons including the baryon antitriplet, sextet, and antidecaplet. We also want to mention that the modification of the pion mean fields in the presence of the  $N_c - 1$  valence quarks has another important physical implications. A recent work on the gravitational form factors of the singly heavy baryons indicate that the stability condition or the von Laue condition [18] for the singly heavy baryons can only be satisfied by using the present modified pion mean fields [19].

The present paper is organized as follows: In Section II, we briefly explain the  $\chi$ QSM. Starting from the baryon correlation function, we show how the pion mean-field solution can be obtained. Then we introduce the collective zero-mode quantization of the baryon and derive the collective Hamiltonian. The collective wave functions for the singly heavy baryons are obtained by diagonalizing the Hamiltonian and coupling the SU(3) wave functions to the heavy quark. In Section III, we first discuss the results of the pion mean-field solutions or the soliton profile functions.

We then present the results of the classical masses as functions of the dynamical quark mass and discuss how the pion mean fields influence them. We also show explicitly that the pion mean-field solution does not exist when the number of the valence quarks  $N_c - 2$ . Finally, we present the results of the masses of the singly heavy baryons including the baryon antitriplet, sextet, and antidecaplet. In the final Section, we summarize the present work and draw conclusions.

## II. HEAVY BARYONS IN THE CHIRAL QUARK-SOLITON MODEL

### A. Nucleon correlation function

In the limit of the infinite heavy-quark mass ( $m_Q \rightarrow \infty$ ), heavy quarks inside a singly or doubly heavy baryon can be viewed as a static color source. It means that the heavy quarks play a mere role to make the heavy baryon a color singlet. In order to describe the heavy baryons within the  $\chi$ QSM, we consider the baryon correlation functions consisting of  $N_c - N_Q$  light valence quarks in Euclidean space, where  $N_Q$  ( $N_Q \leq 2$ ) denotes the number of the heavy quarks involved. This is plausible, since the heavy-quark propagators in the limit of  $m_Q \rightarrow \infty$  contribute to the correlation function of the singly or doubly heavy baryon only in a trivial way. Thus, the correlation function of the singly or doubly heavy baryon can be expressed as

$$\begin{aligned} \Pi_B(\mathbf{x} - \mathbf{y}, T) &= \langle \mathcal{J}_B(\mathbf{x}, T/2) \mathcal{J}_B^\dagger(\mathbf{y}, -T/2) \rangle_0 \\ &= \frac{1}{\mathcal{Z}} \int \mathcal{D}U \mathcal{D}\psi^\dagger \mathcal{D}\psi \mathcal{J}_B(\mathbf{0}, T/2) \mathcal{J}_B^\dagger(\mathbf{0}, -T/2) e^{\int d^4x \psi^\dagger (i\cancel{\partial} + iMU\gamma_5 + i\hat{m})\psi}, \end{aligned} \quad (1)$$

where  $\mathcal{Z}$  is the low-energy effective chiral partition function.  $\mathcal{J}_B$  represents the Ioffe-type baryonic current that consists of  $N_c - N_Q$  light valence quarks for a singly or doubly heavy baryon  $B$

$$\mathcal{J}_B(x) = \frac{1}{(N_c - N_Q)!} \varepsilon^{\alpha_1 \dots \alpha_{N_c - N_Q}} \Gamma_{J' J'_3, T T_3}^{\{f_1 \dots f_{N_c - N_Q}\}} \psi_{\alpha_1 f_1}(x) \dots \psi_{\alpha_{N_c - N_Q} f_{N_c - N_Q}}(x), \quad (2)$$

$\alpha_i$  denote color indices.  $\Gamma_{J' J'_3, T T_3}^f$  is a symmetric matrix with flavor and spin indices  $f$ .  $J'$  and  $T$  represent the spin and isospin of the heavy baryon, respectively and  $J'_3$  and  $T_3$  are the corresponding third components of them, respectively. The notation  $\langle \dots \rangle_0$  in (1) stands for the vacuum expectation value.  $M$  designates the dynamical quark mass and the chiral field  $U^{\gamma_5}$  is defined as

$$U^{\gamma_5} = U \frac{1 + \gamma_5}{2} + U^\dagger \frac{1 - \gamma_5}{2}, \quad (3)$$

with

$$U = \exp \left[ i \frac{\pi^a \lambda^a}{f_\pi} \right]. \quad (4)$$

$\pi^a$  represents the pseudo-Nambu-Goldstone(NG) field.  $\hat{m}$  is the mass matrix of the current quarks, which is written as  $\hat{m} = \text{diag}(m_u, m_d, m_s)$ . We assume in the present work isospin symmetry, i.e.  $m_u = m_d$ . Thus, we introduce the average mass of the up and down quarks  $m_0 = (m_u + m_d)/2$ . The strange current quark mass  $m_s$  will be treated perturbatively to linear order. Since we introduce hedgehog ansatz or hedgehog symmetry, we consider the trivial embedding [2]

$$U(\mathbf{r}) = \begin{pmatrix} U_{SU(2)}(\mathbf{r}) & 0 \\ 0 & 1 \end{pmatrix}, \quad (5)$$

where  $\mathbf{n}$  is defined as the normalized radial vector  $\mathbf{n} = \mathbf{r}/r$ , and  $U_{SU(2)} = \exp[i\mathbf{n} \cdot \boldsymbol{\tau} \Theta(r)]$ .  $\boldsymbol{\tau}$  are the Pauli matrices in isospin space.  $\Theta(r)$  denotes the profile function of the soliton, which will be obtained in a self-consistent way by the minimizing procedure.

Integrating over the quark fields, we obtain the following expression of the baryonic correlation function as

$$\Pi_B(\mathbf{x} - \mathbf{y}, T) = \frac{1}{\mathcal{Z}} \Gamma_{J' J'_3, T T_3}^{\{f\}} \Gamma_{J' J'_3, T T_3}^{\{g\}*} \int \mathcal{D}U \prod_{i=1}^{N_c - N_Q} \left\langle \mathbf{x}, T/2, \alpha_i \left| \frac{1}{D(U)} \right| \mathbf{y}, -T/2, \beta_i \right\rangle e^{-S_{\text{eff}}(U)}, \quad (6)$$

where the one-body Dirac operator  $D(U)$  is defined by

$$D(U) = i\gamma_4\partial_4 + i\gamma_k\partial_k + iMU\gamma_5 + i\hat{m}. \quad (7)$$

$S_{\text{eff}}$  represents the effective chiral action written as

$$S_{\text{eff}} = -N_c \text{Tr} \log D(U). \quad (8)$$

Here,  $\text{Tr}$  denotes the functional trace over space-time and all internal spaces. Taking the Euclidean time to be infinity ( $T \rightarrow \infty$ ), we can pick up lowest-lying baryon states from the correlation function [4, 5] as

$$\Pi_B(\mathbf{x} - \mathbf{y}, T) \sim \exp[-(N_c - N_Q)E_{\text{val}} + E_{\text{sea}}T], \quad (9)$$

where  $E_{\text{val}}$  and  $E_{\text{sea}}$  the valence and sea quark energies. However, the mean fields  $U$  being involved in the calculation should be determined. Note that the profile function  $\Theta(r)$  satisfies the boundary conditions at two end points, i.e.  $\Theta(0) = \pi$  and  $\Theta(\infty) = 0$ . The  $SU(2)$  single-quark Hamiltonian  $h_{SU(2)}(U)$  is defined as

$$h_{SU(2)}(U) = i\gamma_4\gamma_i\partial_i - \gamma_4MU_{SU(2)}^\gamma - \gamma_4m_0. \quad (10)$$

Then, the one-body Dirac equation is written as

$$h_{SU(2)}(U)\Phi_n(\mathbf{r}) = E_n\Phi_n(\mathbf{r}), \quad (11)$$

where  $E_n$  denote the eigen-energies of the one-body Hamiltonian  $h_{SU(2)}(U)$ .

## B. Classical equation of motion and self-consistent solution

The classical equation of motion can be derived by minimizing the energy of the classical soliton

$$\frac{\delta}{\delta\Theta(\mathbf{r})}[(N_c - N_Q)E_{\text{val}} + E_{\text{sea}}] \Big|_{\Theta_c} = 0, \quad (12)$$

where  $\Theta_c$  is the soliton profile function at the stationary point or the pion mean-field solution. Solving Eq. (12), we find the equation of motion

$$\sin\Theta(\mathbf{r})S(\mathbf{r}) - \cos\Theta(\mathbf{r})P(\mathbf{r}) = 0, \quad (13)$$

where  $S(\mathbf{r})$  and  $P(\mathbf{r})$  are defined as

$$\begin{aligned} S(\mathbf{r}) &= M \left[ N_c \sum_n R_2^\Lambda(E_n) \bar{\Phi}_n(\mathbf{r})\Phi_n(\mathbf{r}) + (N_c - N_Q)\theta(E_{\text{val}})\bar{\Phi}_{\text{val}}(\mathbf{r})\Phi_{\text{val}}(\mathbf{r}) \right], \\ P(\mathbf{r}) &= M \left[ N_c \sum_n R_2^\Lambda(E_n) \bar{\Phi}_n(\mathbf{r})i\gamma_5(\tau^i n^i)\Phi_n(\mathbf{r}) + (N_c - N_Q)\theta(E_{\text{val}})\bar{\Phi}_{\text{val}}(\mathbf{r})i\gamma_5(\tau^i n^i)\Phi_{\text{val}}(\mathbf{r}) \right]. \end{aligned} \quad (14)$$

Here,  $\Phi_{\text{val}}(\mathbf{r}) = \langle \mathbf{r} | \text{val} \rangle$  and  $\Phi_n(\mathbf{r}) = \langle \mathbf{r} | n \rangle$  denote the single-particle wave functions of the valence and sea quarks with the corresponding eigen-energies  $E_{\text{val}}$  and  $E_n$  of the one-body Hamiltonian  $h_{SU(2)}(U_c)$ , respectively. The regularization function  $R_2^\Lambda(E_n)$  is defined as

$$R_2^\Lambda(E_n) = \frac{1}{4\sqrt{\pi}} \int \phi(u) \frac{du}{u^{1/2}} E_n e^{-uE_n^2}, \quad (15)$$

where  $\phi(u) = c\theta(u - \Lambda_1^{-2}) + (1 - c)\theta(u - \Lambda_2^{-2})$  [7]. The values of the parameters are taken from Ref. [10]. Thus, the soliton mass is finally derived as

$$M_{\text{sol}} = (N_c - N_Q)\theta(E_{\text{val}})E_{\text{val}}(U_c) + E_{\text{sea}}(U_c). \quad (16)$$

When  $N_Q = 0$ , the result of  $M_{\text{sol}}$  is the same as in the original  $\chi$ QSM for the light baryons. However, when  $N_Q = 1$ , we obtain the modified pion mean-field solutions for the singly heavy baryons. Note that in Ref. [10] the pion mean

fields are assumed to be not changed. In the present work, we will show explicitly that it was not a correct assumption. As for the case of  $N_Q = 2$ , we find that there are no pion mean-field solutions. It implies that the present scheme of the mean-field approach does not apply to the description of doubly heavy baryons. When the dynamical quark mass is almost two times larger than its usual value ( $M \simeq 400$  MeV), we can find the solution of Eq. (13). When  $N_Q \neq 0$ , the classical mass is changed to be

$$M_{\text{cl}} = M_{\text{sol}} + N_Q m_Q, \quad (17)$$

where  $m_Q$  is the *effective* heavy quark mass that contains also the binding energy of the heavy quark. Thus, it is different from that discussed in QCD and will be absorbed in the center mass of each representation, which will be discussed later. Note that when the level of the valence quarks crosses the line where the valence energy becomes negative, the soliton mass is given solely by the sea-quark energy.

### C. Zero-mode collective quantization

Having carried out the zero-mode quantization [5], we arrive at the collective Hamiltonian for singly heavy baryons

$$H = H_{\text{sym}} + H_{\text{sb}}^{(1)}, \quad (18)$$

where  $H_{\text{sym}}$  represents the flavor SU(3) symmetric part

$$H_{\text{sym}} = M_{\text{cl}} + \frac{1}{2I_1} \sum_{i=1}^3 \hat{J}_i^2 + \frac{1}{2I_2} \sum_{a=4}^7 \hat{J}_a^2. \quad (19)$$

Here,  $I_1$  and  $I_2$  denote the moments of inertia of the soliton. The explicit expressions for  $I_{1,2}$  are given in Ref. [5, 7]. Note that the second and third terms in Eq. (19) arise from the rotation of the chiral soliton, which is of order  $1/N_c$  ( $I_{1,2} \sim N_c$ ). The operators  $\hat{J}_i$  and  $\hat{J}_a$  represent the spin generators in SU(3). In the  $(p, q)$  representation of the SU(3) group, we find the eigenvalue of the SU(3) quadratic Casimir operator  $\sum_{i=1}^8 J_i^2$  as

$$C_2(p, q) = \frac{1}{3} [p^2 + q^2 + pq + 3(p + q)]. \quad (20)$$

Thus, the eigenvalues of  $H_{\text{sym}}$  are obtained as

$$E_{\text{sym}}(p, q) = M_{\text{cl}} + \frac{1}{2I_1} J(J + 1) + \frac{1}{2I_2} [C_2(p, q) - J(J + 1)] - \frac{3}{8I_2} Y'^2. \quad (21)$$

The right hypercharge  $Y'$  is constrained to be  $(N_c - N_Q)/3$ , which is imposed by the  $N_c - N_Q$  valence quarks inside a singly heavy baryon. Thus,  $Y'$  counts effectively the number of the valence quarks involved. Note that in the Skyrme model the right hypercharge is constrained by the Wess-Zumino term. When  $Y' = 1$  with  $N_Q = 0$ , i.e. when the light baryons are concerned, it provides the selection rule. That is, only the baryon representations that contain  $Y = 1$  are allowed such as the baryon octet (**8**), decuplet (**10**), antidecuplet ( **$\bar{10}$** ), eikosiheptaplet (**27**), etc., all of which contain the baryons with  $Y = 1$ . When it comes to the singly heavy baryons, the right hypercharge becomes  $Y' = 2/3$ . Thus, allowed representations are the baryon antitriplet ( **$\bar{3}$** ), sextet (**6**) with  $J = 1/2$  and  $J = 3/2$ , antidecapentaplet ( **$\bar{15}$** ) with  $J = 1/2$  and  $J = 3/2$ , etc., which include the singly heavy baryons with  $Y = 2/3$ .

The collective wavefunctions of the baryons are derived as

$$\psi_B^{(\mathcal{R})}(J' J'_3, J; A) = \sqrt{\dim(p, q)} (-1)^{-\frac{Y'}{2} + J_3} D_{(Y, T, T_3)(\bar{Y}, J, -J_3)}^{(\mathcal{R})*}(A), \quad (22)$$

where

$$\dim(p, q) = (p + 1)(q + 1) \left( 1 + \frac{p + q}{2} \right). \quad (23)$$

$J$  stands for the soliton spin, and  $J_3$  represents its third component, respectively.

### D. Collective Hamiltonian for flavor SU(3) symmetry breaking

The symmetry-breaking part of the collective Hamiltonian is given as [5, 7]

$$H_{\text{sb}}^{(1)} = \frac{\Sigma \pi N m_s}{m_0} \frac{1}{3} + \alpha D_{88}^{(8)} + \beta \hat{Y} + \frac{\gamma}{\sqrt{3}} \sum_{i=1}^3 D_{8i}^{(8)} \hat{J}_i, \quad (24)$$

where

$$\alpha = \left( -\frac{\Sigma \pi N}{3m_0} + \frac{K_2}{I_2} Y \right) m_s, \quad \beta = -\frac{K_2}{I_2} m_s, \quad \gamma = 2 \left( \frac{K_1}{I_1} - \frac{K_2}{I_2} \right) m_s. \quad (25)$$

The first term in Eq. (24) can be absorbed into the symmetric part of the Hamiltonian, since it does not contribute to the mass splittings of the baryons in a given representation. The three parameters  $\alpha$ ,  $\beta$ , and  $\gamma$  are expressed in terms of the moments of inertia  $I_{1,2}$  and  $K_{1,2}$ . Since we have  $N_c - N_Q$  light quarks in the case of the heavy baryons, we need to modify the valence contributions to the moments of inertia and the sigma  $\pi N$  term. The modification can be done easily by replacing the prefactor  $N_c$ , which counts the number of the valence quarks, by  $N_c - N_Q$ . The explicit expressions for the moments of inertia and the  $\pi N$  sigma term can be found in Ref. [10].

The effects of flavor SU(3) symmetry breaking being introduced, the collective wavefunctions are no longer expressed by a pure representation but are mixed with other representations. Dealing with the collective Hamiltonian (24) as a small perturbation and using the second-order perturbation theory, we obtain the wavefunctions for the baryon anti-triplet ( $J = 0$ ) and the sextet ( $J = 1$ ) respectively [10] as

$$\begin{aligned} |B_{\bar{3}_0}\rangle &= |\bar{\mathbf{3}}_0, B\rangle + p_{15}^B |\bar{\mathbf{15}}_0, B\rangle, \\ |B_{\mathbf{6}_1}\rangle &= |\mathbf{6}_1, B\rangle + q_{15}^B |\bar{\mathbf{15}}_1, B\rangle + q_{24}^B |\mathbf{24}_1, B\rangle, \end{aligned} \quad (26)$$

with the mixing coefficients

$$p_{15}^B = p_{\bar{15}} \begin{bmatrix} -\sqrt{15}/10 \\ -3\sqrt{5}/20 \end{bmatrix}, \quad q_{15}^B = q_{\bar{15}} \begin{bmatrix} \sqrt{5}/5 \\ \sqrt{30}/20 \\ 0 \end{bmatrix}, \quad q_{24}^B = q_{\bar{24}} \begin{bmatrix} -\sqrt{10}/10 \\ -\sqrt{15}/10 \\ -\sqrt{15}/10 \end{bmatrix}, \quad (27)$$

respectively, in the basis  $[\Lambda_Q, \Xi_Q]$  for the anti-triplet and  $[\Sigma_Q (\Sigma_Q^*), \Xi'_Q (\Xi_Q^*), \Omega_Q (\Omega_Q^*)]$  for the sextets. The expressions for the parameters  $p_{\bar{15}}$ ,  $q_{\bar{15}}$ , and  $q_{\bar{24}}$  are also found in Refs. [10, 11]. Note that the mixing coefficients are proportional to  $m_s$  linearly.

The complete wavefunction for a heavy baryon can be constructed by coupling the soliton wavefunction to the heavy quark such that the heavy baryon becomes a color singlet, which is expressed as

$$|B_\mu; (J', J'_3)(T, T_3)\rangle = \sum_{J_3, J_{Q3}} C_{J, J_3, J_Q, J_{Q3}}^{J' J'_3} \chi_{J_{Q3}} |B_\mu; (J, J_3)(T, T_3)\rangle. \quad (28)$$

Here,  $\chi_{J_{Q3}}$  denotes the heavy-quark spinor and  $C_{J, J_3, J_Q, J_{Q3}}^{J' J'_3}$  represent the corresponding Clebsch-Gordan coefficients.  $|B_\mu; (J, J_3)(T, T_3)\rangle$  means the collective wavefunctions of the quantized light soliton, given already in Eq. (22).

### E. Baryon antitriplet and sextet

Taking into account the  $m_s$  corrections to the first order, we can write the masses of the singly heavy baryons in representation  $\mathcal{R}$  as

$$M_{B, \mathcal{R}}^Q = M_{\mathcal{R}}^Q + M_{B, \mathcal{R}}^{(1)}, \quad (29)$$

where

$$M_{\mathcal{R}}^Q = M_{\text{cl}} + E_{\text{sym}}(p, q). \quad (30)$$

$M_{\mathcal{R}}^Q$  is called the center mass of a heavy baryon in representation  $\mathcal{R}$ .  $E_{\text{sym}}(p, q)$  is defined in Eq. (21). The lower index  $B$  denotes a certain baryon belonging to a specific representation  $\mathcal{R}$ . The upper index  $Q$  stands for either the charm sector ( $Q = c$ ) or the bottom sector ( $Q = b$ ). The center masses for the anti-triplet and sextet representations can be explicitly written as

$$M_{\bar{\mathbf{3}}}^Q = M_{\text{cl}} + \frac{1}{2I_2}, \quad M_{\mathbf{6}}^Q = M_{\bar{\mathbf{3}}}^Q + \frac{1}{I_1}, \quad (31)$$

where  $M_{\text{cl}}$  was defined in Eq. (17). Note that the mass splitting between the baryon anti-triplet and sextet are determined by  $1/I_1 = 178 \text{ MeV}$  in the model, while the experimental data [9, 20] suggest  $1/I_1 \approx 172 \text{ MeV}$ . The second term in Eq. (29) denotes the linear-order  $m_s$  corrections to the heavy baryon mass

$$M_{B, \mathcal{R}}^{(1)} = \langle B, \mathcal{R} | H_{\text{sb}}^{(1)} | B, \mathcal{R} \rangle = Y \delta_{\mathcal{R}}, \quad (32)$$

where

$$\delta_{\bar{\mathbf{3}}} = \frac{3}{8}\alpha + \beta, \quad \delta_{\mathbf{6}} = \frac{3}{20}\alpha + \beta - \frac{3}{10}\gamma. \quad (33)$$

The values of the matrix elements for the relevant SU(3) Wigner  $D$  functions are tabulated in Ref. [10]. Thus, we obtain the masses of the lowest-lying singly heavy baryons as

$$M_{B, \bar{\mathbf{3}}}^Q = M_{\bar{\mathbf{3}}}^Q + Y \delta_{\bar{\mathbf{3}}}, \quad M_{B, \mathbf{6}}^Q = M_{\mathbf{6}}^Q + Y \delta_{\mathbf{6}}, \quad (34)$$

with the linear-order  $m_s$  corrections taken into account.

While the baryon sextet with  $J' = 1/2$  and  $J' = 3/2$  are degenerate in the limit of the infinitely heavy-quark mass ( $m_Q \rightarrow \infty$ ), the degeneracy is removed in reality. Thus, we need to introduce the hyperfine interaction that will lift the degeneracy of different spin states in the sextet representation. This interaction is introduced phenomenologically. So, we will fix the hyperfine interactions by using the experimental data, as was proposed by Ref. [9]. The spin-spin interaction Hamiltonian is written as

$$H_{\text{sol}Q} = \frac{2}{3} \frac{\kappa}{m_Q M_{\text{sol}}} \mathbf{J} \cdot \mathbf{J}_Q = \frac{2}{3} \frac{\varkappa}{m_Q} \mathbf{J} \cdot \mathbf{J}_Q, \quad (35)$$

where  $\kappa$  represents the flavor-independent hyperfine coupling constant. Note that the baryon anti-triplet does not acquire any contribution from the hyperfine interaction, since the corresponding soliton has spin  $J = 0$ . On the other hand, the baryon sextet has  $J = 1$ . Being coupled to the heavy quark spin, it produces two different multiplets, i.e.,  $J' = 1/2$  and  $J' = 3/2$ , of which the masses are expressed respectively as

$$M_{B, \mathbf{6}_{1/2}}^Q = M_{B, \mathbf{6}}^Q - \frac{2}{3} \frac{\varkappa}{m_Q}, \quad M_{B, \mathbf{6}_{3/2}}^Q = M_{B, \mathbf{6}}^Q + \frac{1}{3} \frac{\varkappa}{m_Q}. \quad (36)$$

Thus, we find the hyperfine mass splitting as

$$M_{B, \mathbf{6}_{3/2}}^Q - M_{B, \mathbf{6}_{1/2}}^Q = \frac{\varkappa}{m_Q}, \quad (37)$$

where the corresponding numerical value can be determined by using the center value of the sextet masses. In the charmed and bottom baryon sectors, we obtain the corresponding numerical values respectively

$$\frac{\varkappa}{m_c} = 68.1 \text{ MeV}, \quad \frac{\varkappa}{m_b} = 20.3 \text{ MeV}, \quad (38)$$

which were already shown in Ref. [9].

## F. Heavy pentaquarks

The five resonances of the  $\Omega_c$  were reported by the LHCb [13] Collaboration, of which the four  $\Omega_c$ 's were confirmed by the Belle [14] Collaboration. In a recent work [15],  $\Omega_c(3050)$  and  $\Omega_c(3119)$  with very small decay width among the five  $\Omega_c$ 's were identified as heavy pentaquarks belonging to the baryon antidecapentaplet. The baryon  $\bar{\mathbf{15}}$  was originally proposed by Diakonov [8], since it appears naturally from the  $\chi$ QSM with  $Y = 2/3$ . In the present work,

we compute the mass splittings of the baryon antidecaplet self-consistently. Being similar to the baryon sextet, the antidecaplet consists of the two representations with spin  $J' = 1/2$  and  $J' = 3/2$ .

The expression of the mass formulae of the heavy pentaquarks comes from Eq. (29). The center-mass formulae of the antidecaplet are expressed as

$$\begin{aligned} M_{\overline{\mathbf{15}}, J=0}^Q &= M_{\text{cl}} + \frac{5}{2} \frac{1}{I_2} = M_{\overline{\mathbf{3}}}^Q + \frac{2}{I_2}, \\ M_{\overline{\mathbf{15}}, J=1}^Q &= M_{\text{cl}} + \frac{3}{2} \frac{1}{I_2} + \frac{1}{I_1} = M_{\overline{\mathbf{6}}}^Q + \frac{1}{I_2}, \end{aligned} \quad (39)$$

The value of the moment of inertia  $I_2$  will be explicitly given in Table I later, i.e.  $1/I_2 = 379$  MeV. Note that its value is smaller than with that of  $1/I_2 = 400 - 450$  MeV, which was obtained in Ref. [15].

As mentioned previously, there are two baryon  $\overline{\mathbf{15}}$  representations with spin  $J' = 1/2$  and  $J' = 3/2$ , which are degenerate in the limit of  $m_Q \rightarrow \infty$ . Thus, we need to introduce the same hyperfine interaction given in Eq. (35) to remove the degeneracy. The explicit expressions of the center masses are then given as

$$\begin{aligned} M_{B, \overline{\mathbf{15}}_{1/2}, J=0}^Q &= M_{\overline{\mathbf{3}}}^Q + \frac{2}{I_2}, \\ M_{B, \overline{\mathbf{15}}_{1/2}, J=1}^Q &= M_{\overline{\mathbf{6}}}^Q + \frac{1}{I_2} - \frac{2}{3} \frac{\varkappa}{m_Q}, \\ M_{B, \overline{\mathbf{15}}_{3/2}, J=1}^Q &= M_{\overline{\mathbf{6}}}^Q + \frac{1}{I_2} + \frac{1}{3} \frac{\varkappa}{m_Q}. \end{aligned} \quad (40)$$

The mass splittings within a representation are caused by the linear-order  $m_s$  contributions to the masses of the baryon antidecaplet. The expressions of the  $m_s$  are listed in Table I.

TABLE I.  $m_s$  corrections to the masses of the baryon antidecaplet

$B$	$M_{B, \overline{\mathbf{15}}_{J=0}}^{(1)}$	$M_{B, \overline{\mathbf{15}}_{J=1}}^{(1)}$
$B_Q$	$\frac{1}{4}\alpha + \frac{5}{3}\beta$	$\frac{1}{8}\alpha + \frac{5}{3}\beta - \frac{1}{4}\gamma$
$\Sigma_Q$	$\frac{2}{3}\beta$	$\frac{1}{12}\alpha + \frac{2}{3}\beta - \frac{1}{6}\gamma$
$\Lambda_Q$	$\frac{1}{4}\alpha + \frac{2}{3}\beta$	$\frac{2}{3}\beta$
$\Xi_Q$	$\frac{1}{8}\alpha - \frac{1}{3}\beta$	$-\frac{1}{12}\alpha - \frac{1}{3}\beta + \frac{1}{6}\gamma$
$\Xi_Q^{3/2}$	$-\frac{1}{4}\alpha - \frac{1}{3}\beta$	$\frac{1}{24}\alpha - \frac{1}{3}\beta - \frac{1}{12}\gamma$
$\Omega_Q$	$-\frac{4}{3}\beta$	$-\frac{1}{6}\alpha - \frac{4}{3}\beta + \frac{1}{3}\gamma$

### III. RESULT AND DISCUSSION

The  $\chi$ QSM contains basically three parameters, i.e. the current quark masses  $m_0$  and  $m_s$ , the cut-off masses for the proper-time regularization of the quark loops, the pion decay constant  $f_\pi$ , and the dynamical quark mass  $M$ . In Ref. [7], it was shown how to fix them.  $m_0$  and the cut-off masses are fixed by reproducing the experimental data of the pion mass  $m_\pi = 139.57$  MeV and the pion decay constant  $f_\pi = 93$  MeV, respectively. The strange current quark mass can be also determined by reproducing the kaon mass. However, we will fix it to be  $m_s = 180$  MeV by using the mass splittings of the baryon octet. The dynamical quark mass is considered to be a free parameter. However, it is determined to be  $M = 420$  MeV such that the electric charge radius of the proton is reproduced. Though the parameters  $\varkappa/m_Q$  were introduced phenomenologically, their values were already fixed by the splitting between the baryon sextet representations with  $J' = 1/2$  and  $J' = 3/2$ . Thus, we have no more free parameter to fit in the present work.

To derive the profile function  $\Theta(r)$ , we first have to solve the classical equation of motion (13) self-consistently. Using a trial profile function, for which we use either the linear profile function or the arctangent one, we solve the one-body Dirac equation (11), so that we obtain the eigen-energies and eigenfunctions of the valence and sea quarks. Inserting them into Eq. (14) and solving Eq. (13), we find a new profile function. We repeat this process until we obtain the classical energy, which converges enough. This is nothing but a well-known Hartree approximation. In the left panel of Fig. 1, we draw the results of the self-consistent profile functions for both the light and singly heavy baryons with



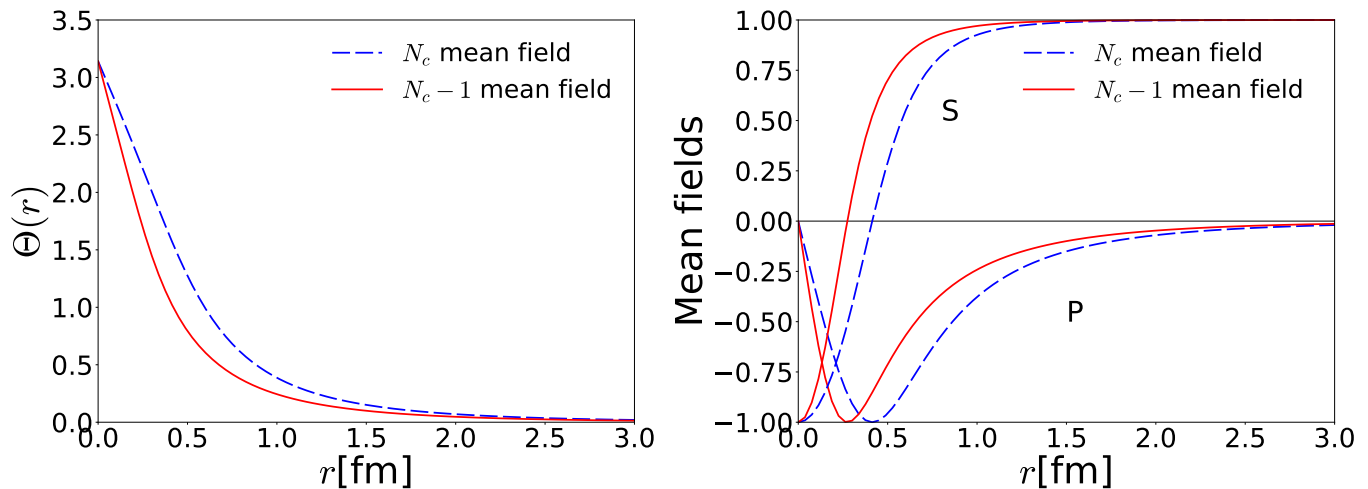


FIG. 1. The results of the self-consistent profile functions  $\Theta(r)$  in the left panel and those of the self-consistent scalar and pseudoscalar mean fields in the right panel. The dashed curves depict the results for the light baryons, whereas the solid ones draw those for the singly-heavy baryons. The value of the dynamical quark mass  $M = 420$  MeV is used.

$M = 420$  MeV used. The dashed curves exhibit that for the light baryons and the solid ones show that for the singly heavy baryons. As for the doubly heavy baryons,  $M = 420$  MeV is not strong enough to find the minimum solution of the classical equation of motion. As will be discussed later, a solution for the doubly heavy baryons only appears when  $M$  is larger than around 600 MeV. As shown in the left panel of Fig. 1, the profile function for the singly heavy baryons shrinks from that for the light baryons. Since the number of the light quarks inside a singly heavy baryon is less than that inside a light baryon, the strength of the pion mean fields is weakened. As a result, the size of the soliton is also decreased. The soliton size is around 0.6 fm for the light baryons with  $N_c = 3$ , whereas it is around 0.4 fm for the singly heavy baryons. In the right panel of Fig. 1, we draw the scalar and pseudoscalar mean fields  $S(r)$  and  $P(r)$ , which are defined in Eq. (14). As expected from the results of the profile functions, the scalar and pseudoscalar mean-field densities are also shifted to the core of the soliton.

We want to emphasize that the soliton for the  $N_c - 1$  valence quarks is naturally the bosonic one, whereas that for the  $N_c$  is the fermionic one. This is a unique feature of the  $\chi$ QSM, which is distinguished from any topological chiral soliton models, including the Skyrme models, where the baryon number is identified with the topological winding number or topological charge from the Wess-Zumino term. In the Skyrme models, the integer winding number is essential to have a finite energy for a stable topological soliton. On the other hand, we do not need to have the integer winding number, since the baryon number is constrained by the valence quarks. The baryon number of the singly heavy baryon will be given by the  $N_c - 1$  light valence quarks together with a heavy quark. This is a distinguished feature from a Skyrme model for heavy baryons [21]. We will discuss it in more detail later.

In Fig. 2, we draw the soliton mass  $M_{\text{sol}}$  defined in Eq. (16) as a function of the dynamical quark mass  $M$ . The results are the same as in Ref. [5]. When the  $N_c$  valence quarks are present, the mean-field solutions of the classical equation of the motion exist when  $M$  is larger than the critical mass  $M_{\text{cr}} \approx 350$  MeV below which there is no solution. Note that the dynamical quark mass plays a role of the coupling between the quark and the pion. So,  $M$  is smaller than  $M_{\text{cr}}$ , the interaction strength is not enough to bind the  $N_c$  valence quarks. As  $M$  increases above  $M_{\text{cr}}$ , the valence-quark energy starts to decrease monotonically, whereas the sea-quark energy increases. It indicates that as  $M$  becomes larger, the vacuum is polarized more strongly. This is very important to stabilize the pion mean-field solution or the chiral soliton. Though the valence- and sea-quark energies depend on  $M$  rather sensitively, the soliton mass decreases rather mildly, as  $M$  increases. When the value of  $M$  is approximately 800 MeV, the valence level crosses the line, below which the valence-quark energy turns negative. Then, the soliton mass is only given by the sea-quark energy. In this case, the baryon number is identified with the winding number. If we further increase  $M$ , the valence level may dive into the negative Dirac sea. This corresponds to the Skyrme picture of the baryon as a topological soliton. This can be justified by the gradient expansion. If  $M > 1$  GeV and the soliton rotates slowly,

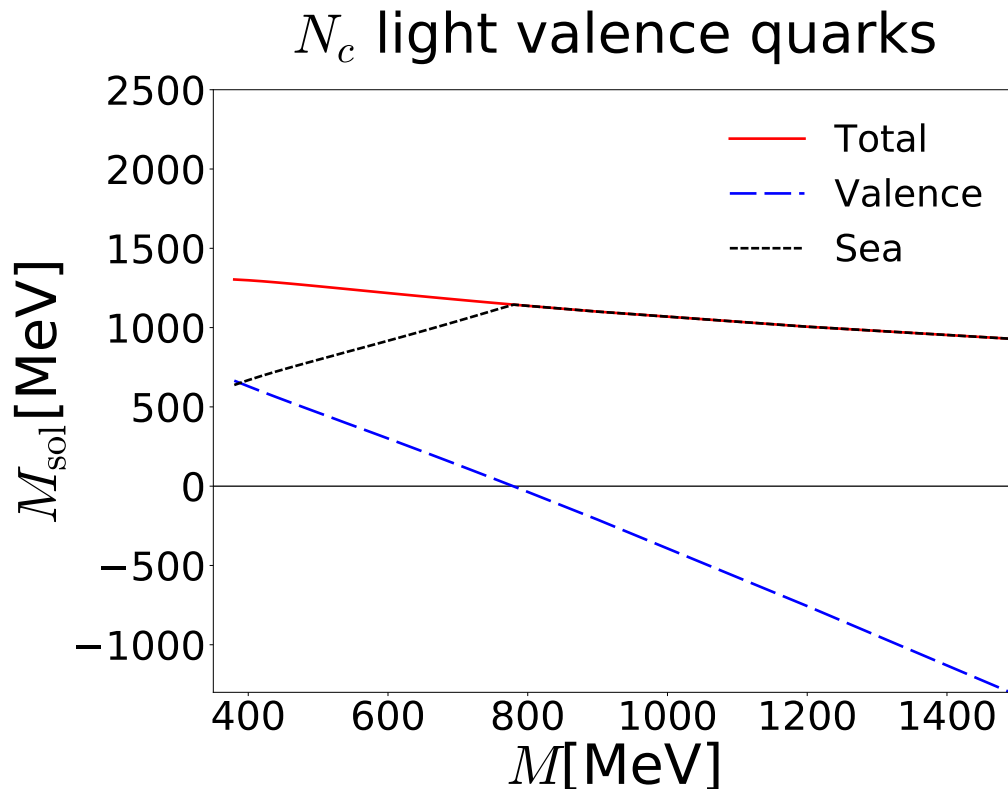


FIG. 2. Soliton mass as a function of the dynamical quark mass  $M$  for the  $N_c$  mean field. The long-dashed line draws the valence-quark contribution, whereas the short-dashed one depicts the sea-quark contribution. The solid line represents the soliton mass.

then  $\partial_k U/M$  becomes small. Hence, it can be used as an expansion parameter to expand the baryon charge [4]

$$\begin{aligned}
 B(U) &= - \int \frac{d\omega}{2\pi} \text{Tr} \left( \frac{1}{i\omega + h_{\text{SU}(2)}(U)} - \frac{1}{i\omega + h_0} \right) \\
 &= - \int \frac{d\omega}{2\pi} \text{Tr} \left( \frac{h_{\text{SU}(2)}(U)}{\omega^2 + h_{\text{SU}(2)}^2(U)} - \frac{h_0}{\omega^2 + h_0^2} \right),
 \end{aligned} \tag{41}$$

where  $h_0$  is the Dirac Hamiltonian with the  $U$  field turned off.  $h_{\text{SU}(2)}^2(U)$  and  $h_0^2$  are written respectively as

$$h_{\text{SU}(2)}^2 = -\partial_k^2 + M^2 + iM\gamma_k \partial_k U \gamma_5, \quad h_0^2 = -\partial_k^2 + M^2. \tag{42}$$

The leading term of the gradient term is obtained to be

$$B(U) = -\frac{1}{24\pi^2} \varepsilon_{ijk} \text{Tr} [(U^\dagger \partial_i U)(U^\dagger \partial_j U)(U^\dagger \partial_k U)], \tag{43}$$

which is the well-known expression for the winding number in the Skyrme model [22]. Thus, when  $M$  becomes very large ( $M > 1$  GeV), one can see that the nucleon arises as a topological soliton. We will see that in the case of the  $N_c - 1$  the mean-field solution reveals a remarkable feature when  $M$  increases.

Figure 3 illustrates the soliton mass for the  $N_c - 1$  mean fields, i.e., for the singly heavy baryons, as a function of  $M$ . Note that in this case the soliton is the bosonic one consisting of two valence quarks with  $N_c = 3$ , as already mentioned previously. Since the number of the valence quarks are reduced by one, we expect that the Dirac-sea polarization becomes weaker than the case of the three valence quarks. Indeed, the solitonic solution exists only when the dynamical quark mass is larger than  $M_{\text{cr}} \approx 400$  MeV, as shown in Fig. 3. The general tendency of the valence- and sea-quark energies is similar to the case of the  $N_c$  mean field. However, the sea-quark energy increases faster than the rate that the valence-quark one falls off as  $M$  increases. As a result, the soliton mass rises monotonically very mildly. However, when the valence-quark level crosses the line at which the valence energy vanishes, the soliton mass

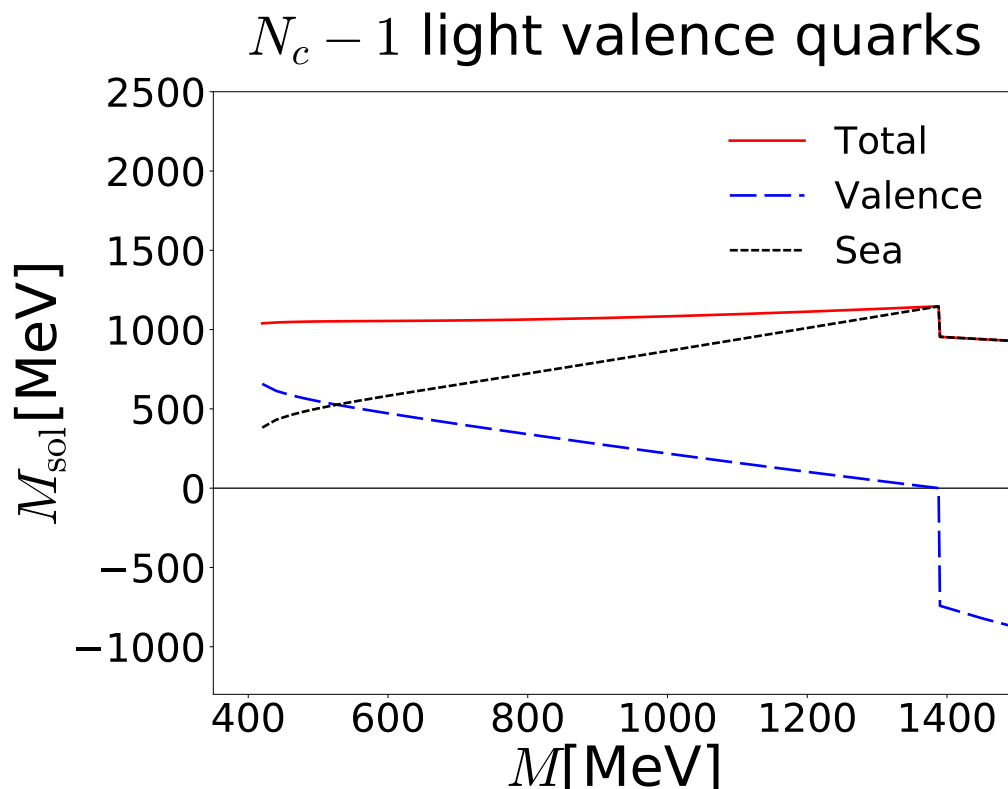


FIG. 3. Soliton mass as a function of the dynamical quark mass  $M$  for the  $N_c - 1$  mean fields. The long-dashed line draws the valence-quark contribution, whereas the short-dashed one depicts the sea-quark contribution. The solid line represents the soliton mass.

coincides exactly with the that of the  $N_c$  mean field. This can be understood by Eq. (16). The soliton mass comes solely from the sea-quark energy. Moreover, in this case, the baryon number is acquired by the winding number as we discussed previously. Thus, the present picture is reduced to the Skyrme model for the singly heavy baryons [21], where the singly heavy baryons were constructed by putting together the topological soliton with the baryon number  $B = 1$  and a heavy meson. However, we emphasize again that singly heavy baryons arise from the  $N_c - 1$  bosonic soliton together with a heavy quark when the plausible value of  $M$  is used.

In Fig. 4 we draw the soliton mass for the  $N_c - 2$  mean fields. In this case, the soliton is just a qualiton consisting of a single light valence quark. Unfortunately, the solitonic solution does not exist with the dynamical quark mass  $M = 420$  MeV we adopt. The mean-field solution only appears when  $M$  is larger than  $M \approx 600$  MeV. Though  $N_c - 2$  is parametrically large, we have in practice only one valence quark. Thus, we are not able to study the doubly heavy baryons within the present approach. A single valence quark is not enough to form a soliton with the proper value of the dynamical quark mass.

In Table II, we list in the second column the results of the moments of inertia, sigma  $\pi N$  term, and the classical soliton mass  $M_{\text{sol}}$  for the  $N_c$  soliton. In the last column, the results of the same quantities are listed for the  $N_c - 1$  soliton. Note that in the case of the  $N_c - 1$  mean fields, the valence parts of these quantities have  $N_c - 1$  factors instead of  $N_c$ . What is interesting is that, naively thinking, valence part of the moments of inertia with  $N_c - 1$  factors would decrease in comparison with the results of those in the case of the  $N_c$  mean fields. However, the situation is more complicated and dynamical. As shown in Table II, the results of the valence parts of the moments of inertia increase in comparison with the case of the  $N_c$  mean fields, whereas those of the sea parts of them decrease by changing the mean fields from  $N_c$  to  $N_c - 1$ . The total results of  $I_1$  and  $I_2$  with the  $N_c - 1$  mean fields are rather similar to those with  $N_c$  ones. On the other hand, the total results of the anomalous moments of inertia  $K_1$  and  $K_2$  with the  $N_c - 2$  mean fields, which arise from the linear  $m_s$  corrections, become larger than those with  $N_c$  mean fields. The  $\bar{\Sigma}_{\pi N}$  and  $M_{\text{sol}}$  with  $N_c - 1$  mean fields are smaller than those with  $N_c$  ones.

Since the  $\bar{\Sigma}_{\pi N}$  is proportional to the matrix element  $\langle n | \gamma_4 | n \rangle$  as shown in Eq. (A2), it is easy to understand that the value of  $\bar{\Sigma}_{\pi N}$  becomes smaller than that of  $\Sigma_{\pi N}$ . It is also natural that  $M_{\text{sol}}$  with the  $N_c - 1$  mean fields turn out smaller than that with the  $N_c$  mean fields (see Eq. (16)). However, when it comes to the moments of inertia, the

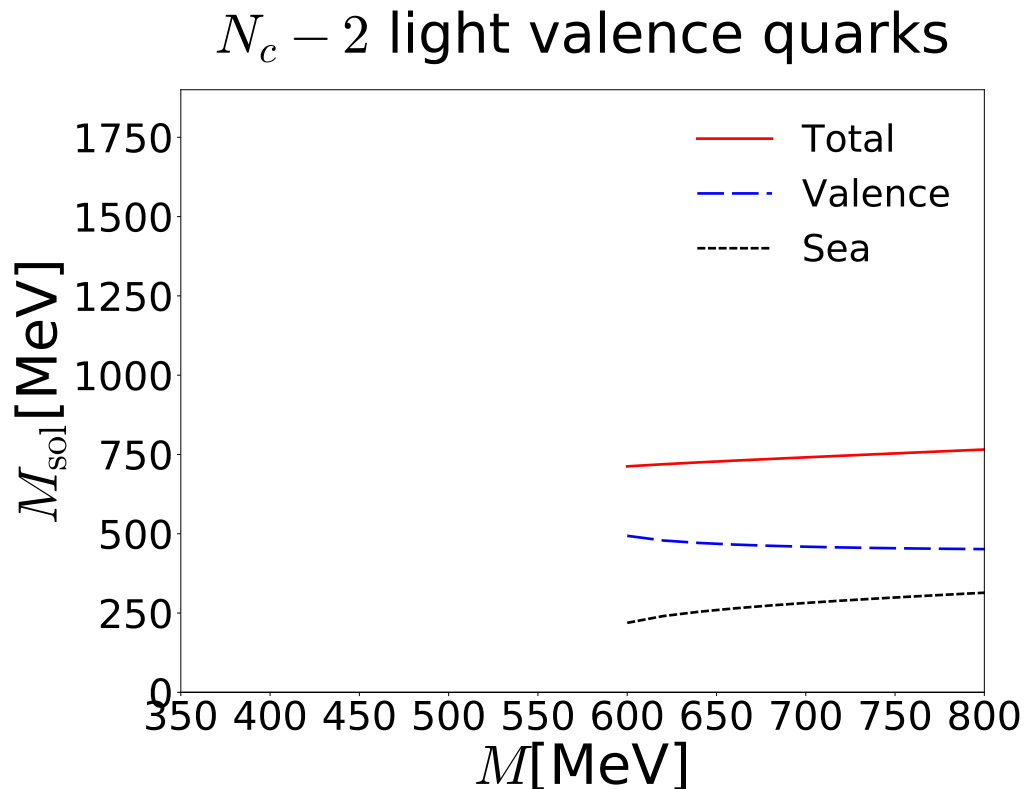


FIG. 4. Soliton mass as a function of the dynamical quark mass  $M$  for the  $N_c - 2$  mean fields. The long-dashed line draws the valence-quark contribution, whereas the short-dashed one depicts the sea-quark contribution. The solid line represents the soliton mass.

denominators  $E_n - E_{\text{val}}$  and  $E_n - E_m$  with  $N_c - 1$  mean fields in Eqs. (A7) and (A11) become smaller than those with  $N_c$  mean fields, which brings about the increase of the values of the moments of inertia.

In Table III, we list the numerical results of the dynamical parameters  $\alpha$ ,  $\beta$ , and  $\gamma$  in Eq. (25) in comparison with the previous works. Those of  $\delta_{\bar{3}}$  and  $\delta_{\bar{3}}$  in Eq. (33) are also presented. The results are compared with those of the previous work [10], in which the  $N_c$  mean fields were used without any modification, assuming that the mean fields would not be much changed. However, as shown in Table III, the results of  $\alpha$ ,  $\beta$ , and  $\gamma$  turn out to be much different from those of Ref. [10]. What is more interesting is that the results of  $\delta_{\bar{3}}$  and  $\delta_{\bar{3}}$  are much closer to those extracted from the experimental data, compared even with those of Ref. [9], in which all the dynamical parameters were determined by the experimental data on the light baryons. Note that since Ref. [9] performed a “model-independent” analysis, it is not possible to decompose the valence-quark and sea-quark parts. To compensate this, an additional scale factor was introduced in Ref. [9]. Thus, the  $N_c - 1$  mean fields derived in the present work provide not only a theoretically consistent method but also a phenomenologically better description of the experimental data.

In Table IV, we list the numerical results of the masses of the lowest-lying charmed baryons, comparing them with those of Ref. [9, 10]. Note that in Ref. [10] the center masses were rather different from the experimental data. Thus, the relevant parameters had to be fitted to the data. In the fifth column with [10]\*, we list the results that were reevaluated without fitting the center masses. As can be observed by comparing the present results with those listed in the fifth column, the  $N_c - 1$  pion mean fields describe the experimental data far better than the  $N_c$  mean fields. Even compared with those of the model-independent analysis [9], the present results are quantitatively comparable with those of Ref. [9].

In Table V, we present the numerical results of the masses of the lowest-lying bottom baryons. As in the case of the charmed baryons, the results are in good agreement with the experimental data. The present model predicts the  $\Omega_b^*$  mass to be 6100.1 MeV, which is slightly larger than that of Ref. [9]. Again, this work reproduces quantitatively the data by far better than Ref. [10]\*.

TABLE II. Results of the moments of inertia ( $I_1$ ,  $I_2$ ), the anomalous moments of inertia ( $K_1$ ,  $K_2$ ), the sigma  $\pi N$  terms, and the soliton mass for the  $N_c$  and  $N_c - 1$  mean fields. The dynamical quark mass  $M = 420$  MeV is use. The second column lists the results for the  $N_c$  mean field, whereas the fourth column shows those for the  $N_c - 1$  mean field. Note that  $\bar{\Sigma}_{\pi N}$  denotes the modified sigma  $\pi N$  term. Its valence part is defined as  $\bar{\Sigma}_{\pi N}^{\text{val}} = (N_c - 1)\Sigma_{\pi N}^{\text{val}}/N_c$ . Its sea part is the same as the original sigma  $\pi N$  term.

$N_c$ mean field		$N_c - 1$ mean field	
$I_1^{\text{val}}$ [fm]	0.7923	$I_1^{\text{val}}$ [fm]	0.9591
$I_1^{\text{sea}}$ [fm]	0.3137	$I_1^{\text{sea}}$ [fm]	0.1438
$I_1$ [fm]	1.1060	$I_1$ [fm]	1.1029
$I_2^{\text{val}}$ [fm]	0.3737	$I_2^{\text{val}}$ [fm]	0.4542
$I_2^{\text{sea}}$ [fm]	0.1551	$I_2^{\text{sea}}$ [fm]	0.0657
$I_2$ [fm]	0.5288	$I_2$ [fm]	0.5199
$K_1^{\text{val}}$ [fm]	0.4260	$K_1^{\text{val}}$ [fm]	0.6903
$K_1^{\text{sea}}$ [fm]	0.0009	$K_1^{\text{sea}}$ [fm]	0.0001
$K_1$ [fm]	0.4269	$K_1$ [fm]	0.6904
$K_2^{\text{val}}$ [fm]	0.2741	$K_2^{\text{val}}$ [fm]	0.3665
$K_2^{\text{sea}}$ [fm]	-0.0019	$K_2^{\text{sea}}$ [fm]	-0.0005
$K_2$ [fm]	0.2722	$K_2$ [fm]	0.3660
$\Sigma_{\pi N}^{\text{val}}$ [MeV]	11.07	$\bar{\Sigma}_{\pi N}^{\text{val}}$ [MeV]	8.73
$\Sigma_{\pi N}^{\text{sea}}$ [MeV]	32.92	$\bar{\Sigma}_{\pi N}^{\text{sea}}$ [MeV]	14.49
$\Sigma_{\pi N}$ [MeV]	43.99	$\bar{\Sigma}_{\pi N}$ [MeV]	23.22
$M_{\text{sol}}^{\text{val}}$ [MeV]	595	$M_{\text{sol}}^{\text{val}}$ [MeV]	658
$M_{\text{sol}}^{\text{sea}}$ [MeV]	697	$M_{\text{sol}}^{\text{sea}}$ [MeV]	382
$M_{\text{sol}}$ [MeV]	1292	$M_{\text{sol}}$ [MeV]	1040

TABLE III. Results of the dynamical parameters for the flavor SU(3) symmetry breaking. The strange current quark mass is taken to be  $m_s = 180$  MeV. The results are compared with the previous works [9, 10]. In Ref. [10] all the results were computed without modifying the mean fields. In the last column, the values of  $\delta_{\bar{3}}$  and  $\delta_{\mathbf{6}}$  were listed, which were determined by the experimental data.

[MeV]	This work	[10]	[9]	Experiment [20]
$\alpha$	-142.7	-337.8	-255.03 $\pm$ 5.82	-
$\beta$	-126.7	-80.6	-140.04 $\pm$ 3.20	-
$\gamma$	-28.10	-39.3	-101.08 $\pm$ 2.33	-
$\delta_{\bar{3}}$	-180.3	-207.3	-203.8 $\pm$ 3.5	$\sim$ -182.9
$\delta_{\mathbf{6}}$	-139.7	-119.5	-135.2 $\pm$ 3.3	$\sim$ -122.4

#### IV. SUMMARY AND CONCLUSIONS

In the present work, we investigated how the pion mean fields underwent the changes within the framework of the self-consistent chiral quark-soliton model, when the number of the light valence quarks is reduced from  $N_c$  to  $N_c - N_Q$ . Starting from the baryon correlation functions with  $N_c - 1$  valence quarks, we derived the classical energy of the classical soliton. Having minimized the energy, we found the equation of motion. Having solved it in a self-consistent way, we obtained the numerical result of the profile function for the classical soliton solution or the pion mean fields. Compared with the profile function for the  $N_c$  pion mean fields, that for the  $N_c - 1$  mean fields shrinks to the core of the soliton. We also found that the solution for the  $N_c - 2$  mean fields did not exist with the proper

TABLE IV. Results of the masses of the ground-state charmed baryons in units of MeV in comparison with those of Refs. [9, 10]. The results listed in the fifth column [10]\* are rederived without fitting the center masses to the experimental data. For details, see the related text. The last column lists the experimental data.

$\mathcal{R}_{J'}^Q$	$B_c$	This work	[10]	[10]*	[9]	Experiment [20]
$\bar{\mathbf{3}}_{1/2}^c$	$\Lambda_c$	2278.4	2274.4	2225.4	2272.5±2.3	2286.5±0.1
$\bar{\mathbf{3}}_{1/2}^c$	$\Xi_c$	2458.6	2481.5	2432.7	2476.3±1.2	2469.4±0.3
$\mathbf{6}_{1/2}^c$	$\Sigma_c$	2438.6	2455.7	2472.0	2445.3±2.5	2453.5±0.1
$\mathbf{6}_{1/2}^c$	$\Xi'_c$	2578.3	2575.2	2591.4	2580.5±1.6	2576.8±2.1
$\mathbf{6}_{1/2}^c$	$\Omega_c$	2718.1	2694.6	2711.0	2715.7±4.5	2695.2±1.7
$\mathbf{6}_{3/2}^c$	$\Sigma_c^*$	2506.7	2523.9	2540.1	2513.4±2.3	2518.1±0.8
$\mathbf{6}_{3/2}^c$	$\Xi_c^*$	2646.4	2643.3	2659.6	2648.6±1.3	2645.9±0.4
$\mathbf{6}_{3/2}^c$	$\Omega_c^*$	2786.2	2762.7	2779.1	2783.8±4.5	2765.9±2.0

TABLE V. Results of the masses of the ground-state bottom baryons in units of MeV in comparison with those of Refs. [9, 10]. The results listed in the fifth column [10]\* are rederived without fitting the center masses to the experimental data. For details, see the related text. The last column lists the experimental data.

$\mathcal{R}_{J'}^Q$	$B_b$	This work	[10]	[10]*	[9]	Experiment [20]
$\bar{\mathbf{3}}_{1/2}^b$	$\Lambda_b$	5608.2	5602.7	5554.3	5599.3±2.4	5619.5±0.2
$\bar{\mathbf{3}}_{1/2}^b$	$\Xi_b$	5788.5	5809.9	5761.6	5803.1±1.2	5793.1±0.7
$\mathbf{6}_{1/2}^b$	$\Sigma_b$	5800.3	5812.7	5832.7	5804.3±2.4	5813.4±1.3
$\mathbf{6}_{1/2}^b$	$\Xi'_b$	5940.1	5932.1	5952.2	5939.5±1.5	5935.0±0.05
$\mathbf{6}_{1/2}^b$	$\Omega_b$	6079.8	6051.6	6071.7	6074.7±4.5	6048.0±1.9
$\mathbf{6}_{3/2}^b$	$\Sigma_b^*$	5820.6	5834.7	5853.0	5824.6±2.3	5833.6±1.3
$\mathbf{6}_{3/2}^b$	$\Xi_b^*$	5960.3	5954.2	5972.5	5959.8±1.2	5955.3±0.1
$\mathbf{6}_{3/2}^b$	$\Omega_b^*$	6100.1	6073.6	6092.0	6095.0±4.4	-

value of the dynamical quark mass. It implies that the present scheme is not suitable for the description of the doubly heavy baryons. The soliton mass was also investigated as a function of the dynamical quark mass  $M$ . The solution exists when  $M$  is approximately larger than 400 MeV. As  $M$  increases, the valence-quark contribution falls off slowly whereas the sea-quark contribution increases also mildly. However, when  $M$  reaches around 1390 MeV, where the valence-quark part vanishes, the sea-quark contribution coincides exactly with that of the soliton mass with the  $N_c$  valence quarks. It indicates that when the valence energy crosses the line at which it becomes zero the baryon number is acquired by the winding number or the topological charge as in the case of the Skyrme model. We want to emphasize that the soliton is made of the  $N_c - 1$  valence quarks, i.e. a bosonic soliton with the proper value of the dynamical quark mass, which is conceptually different from any topological chiral soliton models including the Skyrme model.

The moments of inertia and anomalous moments of inertia become larger than those with the  $N_c$  mean fields. The changes from the  $N_c$  to  $N_c - 1$  valence quarks give rise to nontrivial effects on these dynamical quantities of the classical soliton. The results of the masses of the charmed and bottom baryons show that the modification of the pion mean fields reproduce the experimental data much better than the previous work if one does not fit the center masses of the heavy baryons. The  $\Omega_b^*$  baryon is predicted to be  $M_{\Omega_b^*} = 6100.1$  MeV, which is slightly larger than that from the model-independent analysis. We also computed the masses of the charmed and bottom baryon antidecaplet. In general, the present work yield larger values of the masses in comparison with the previous works except for the  $B_c$  baryons.

In conclusion, it is essential to consider the modification of the pion mean fields when the number of the valence quarks is reduced from  $N_c$  to  $N_c - 1$ . The  $N_c - 1$  mean fields provide a better understanding of the nature of the singly heavy baryons and a more quantitative description of the masses of the charmed and bottom baryons than the  $N_c$  pion mean fields. Though the numbers of the valence quarks  $N_c$  and  $N_c - 1$  seem to be parametrically the same,

they yield different results in reality. The  $N_c - 1$  pion mean-field solutions can be also used for the investigation of various observables and form factors of the singly heavy baryons. The corresponding works are under way.

### ACKNOWLEDGMENTS

The present work was supported by Basic Science Research Program through the National Research Foundation of Korea funded by the Ministry of Education, Science and Technology (Grant-No. 2018R1A2B2001752 and 2018R1A5A1025563). J.-Y. Kim is partially supported by a DAAD doctoral scholarship.

### Appendix A: Moments of inertia

In this Appendix, we present all relevant formulae for the modified  $\pi N$  sigma term, the moments of inertia  $I_{1,2}$ ,  $K_{1,2}$ , and  $N_{1,2}$ . The modified  $\pi N$  sigma term is expressed as

$$\bar{\Sigma}_{\pi N} = \bar{\Sigma}_{\pi N}^{\text{val}} + \Sigma_{\pi N}^{\text{sea}}, \quad (\text{A1})$$

where the valence and sea parts are written respectively as

$$\bar{\Sigma}_{\pi N}^{\text{val}} = m_0(N_c - 1)\langle \text{val} | \gamma_4 | \text{val} \rangle, \quad \Sigma_{\pi N}^{\text{sea}} = \frac{m_0}{2} N_c \sum_n \langle n | \gamma_4 | n \rangle \text{sign}(E_n) \mathcal{R}_{\Sigma}(E_n), \quad (\text{A2})$$

where  $\gamma_4$  denotes the Dirac  $\gamma$  matrix in Euclidean space

$$\gamma_4 = \begin{pmatrix} \mathbf{1} & 0 \\ 0 & -\mathbf{1} \end{pmatrix}. \quad (\text{A3})$$

The function  $\mathcal{R}_{\Sigma}(E_n)$  stands for a regulator

$$\mathcal{R}_{\Sigma}(E_n) = \frac{1}{\sqrt{\pi}} \int_0^{\infty} \frac{du}{\sqrt{u}} e^{-u} \phi(u/E_n^2), \quad (\text{A4})$$

where  $\phi(u)$  [7] represents a cutoff function defined by

$$\phi(u) = c\theta(u - 1/\Lambda_1^2) + (1 - c)\theta(u - 1/\Lambda_2^2). \quad (\text{A5})$$

The free parameters  $\Lambda_1$ ,  $\Lambda_2$ , and  $c$  are determined by reproducing the pion decay constant  $f_{\pi} = 93$  MeV and the pion mass  $m_{\pi} = 139$  MeV in the mesonic sector. The corresponding numerical values are explicitly given as  $\Lambda_1 = 381.15$  MeV,  $\Lambda_2 = 1428.00$  MeV, and  $c = 0.7276$ .

The moment of inertia tensor  $I_{ab}$  is given as follows:

$$I_{ab} = I_{ab}^{\text{val}} + I_{ab}^{\text{sea}}, \quad (\text{A6})$$

where

$$I_{ab}^{\text{val}} = \frac{(N_c - 1)}{2} \sum_{\text{val}, n \neq \text{val}} \frac{\langle n | \lambda_a | \text{val} \rangle \langle \text{val} | \lambda_b | n \rangle}{E_n - E_{\text{val}}},$$

$$I_{ab}^{\text{sea}} = \frac{N_c}{4} \sum_{m, n} \langle n | \lambda_a | m \rangle \langle m | \lambda_b | n \rangle \mathcal{R}_I(E_n, E_m), \quad (\text{A7})$$

with the different regulator  $\mathcal{R}_I(E_n, E_m)$

$$\mathcal{R}_I(E_n, E_m) = \frac{1}{2\sqrt{\pi}} \int_0^{\infty} \frac{du}{\sqrt{u}} \phi(u) \left[ \frac{e^{-uE_n^2} - e^{-uE_m^2}}{u(E_m^2 - E_n^2)} - \frac{E_n e^{-uE_n^2} + E_m e^{-uE_m^2}}{E_m + E_n} \right]. \quad (\text{A8})$$

$\lambda_a$  in Eq. (A7) stand for the Gell-Mann matrices for flavor SU(3) group, satisfying the relations  $\text{tr}(\lambda_a \lambda_b) = 2\delta_{ab}$  and  $[\lambda_a, \lambda_b] = 2if_{abc}\lambda_c$ ,  $a = 1, \dots, 8$ . The moments of inertia  $I_1$  and  $I_2$  are defined by

$$I_{ab} \equiv \begin{cases} I_1 \delta_{ab} & a, b = 1, 2, 3 \\ I_2 \delta_{ab} & a, b = 4, 5, 6, 7 \\ 0 & a, b = 8 \end{cases} . \quad (\text{A9})$$

Similarly, the anomalous moments of inertia tensor is written as

$$K_{ab} = K_{ab}^{\text{val}} + K_{ab}^{\text{sea}}, \quad (\text{A10})$$

where

$$K_{ab}^{\text{val}} = \frac{(N_c - 1)}{2} \sum_{\text{val}, n \neq \text{val}} \frac{\langle n | \lambda_a | \text{val} \rangle \langle \text{val} | \lambda_b \gamma_4 | n \rangle}{E_n - E_{\text{val}}},$$

$$K_{ab}^{\text{sea}} = \frac{N_c}{8} \sum_{m, n} \langle n | \lambda_a | m \rangle \langle m | \gamma_4 \lambda_b | n \rangle \frac{\text{sign}(E_n) - \text{sign}(E_m)}{E_n - E_m}. \quad (\text{A11})$$

The anomalous moments of inertia  $K_1$  and  $K_2$  are defined by

$$K_{ab} \equiv \begin{cases} K_1 \delta_{ab} & a, b = 1, 2, 3 \\ K_2 \delta_{ab} & a, b = 4, 5, 6, 7 \\ 0 & a, b = 8 \end{cases} . \quad (\text{A12})$$

### Appendix B: Matrix elements of the SU(3) Wigner $D$ functions

In Appendix B, we tabulate all relevant matrix elements of the SU(3) Wigner  $D$  functions in each representation.

TABLE VI. Matrix elements of the SU(3) Wigner  $D$  functions  $D_{88}^{(8)}$  and  $D_{8i}^{(8)} J_i$ .

	$\mathcal{R}$	T	Y	$\langle \mathcal{R} Y T J   D_{88}^{(8)}   \mathcal{R} Y T J \rangle$	$\langle \mathcal{R} Y T J   D_{8i}^{(8)} J_i   \mathcal{R} Y T J \rangle$
$B_Q$		1/2	5/3	1/4	0
$\Sigma_Q$		1	2/3	0	0
$\Lambda_Q$	$\overline{\mathbf{15}} (J=0)$	0	2/3	1/4	0
$\Xi_Q$		1/2	-1/3	1/8	0
$\Xi_Q^{3/2}$		3/2	-1/3	-1/4	0
$\Omega_Q$		1	-4/3	0	0
$B_Q$		1/2	5/3	1/8	-1/4
$\Sigma_Q$		1	2/3	1/12	-1/6
$\Lambda_Q$	$\overline{\mathbf{15}} (J=1)$	0	2/3	0	0
$\Xi_Q$		1/2	-1/3	-1/12	1/6
$\Xi_Q^{3/2}$		3/2	-1/3	1/24	-1/12
$\Omega_Q$		1	-4/3	-1/6	1/3

### Appendix C: Mass spectra of the baryon antidecaplet

In Appendix C, we present the results for the masses of the baryon antidecaplet for completeness. In Ref. [15], the two of the newly found  $\Omega_c$ 's [13] were interpreted as the  $\Omega_c$ 's that belong to the baryon antidecaplet. As



TABLE VII. Results of the masses of the charmed baryon antidecapentaplet in units of MeV in comparison with those of Ref. [15]. The fourth column lists the results obtained by using the  $N_c$  pion mean fields [10].

$\mathcal{R}_{J'}^Q$	$B_Q$	This work	[10]*	[15]
$\overline{\mathbf{15}}_1^c(J=0)$	$B_c$	2909	3209	-
$\overline{\mathbf{15}}_1^c(J=0)$	$\Sigma_c$	3072	3374	-
$\overline{\mathbf{15}}_1^c(J=0)$	$\Lambda_c$	3036	3290	-
$\overline{\mathbf{15}}_1^c(J=0)$	$\Xi_c$	3181	3413	-
$\overline{\mathbf{15}}_1^c(J=0)$	$\Xi_c^{3/2}$	3234	3539	-
$\overline{\mathbf{15}}_1^c(J=0)$	$\Omega_c$	3325	3536	-
$\overline{\mathbf{15}}_1^c(J=1)$	$B_c$	2682	2952	2685
$\overline{\mathbf{15}}_1^c(J=1)$	$\Sigma_c$	2819	3053	2808
$\overline{\mathbf{15}}_1^c(J=1)$	$\Lambda_c$	2826	3075	2806
$\overline{\mathbf{15}}_1^c(J=1)$	$\Xi_c$	2960	3177	2928
$\overline{\mathbf{15}}_1^c(J=1)$	$\Xi_c^{3/2}$	2949	3145	2931
$\overline{\mathbf{15}}_1^c(J=1)$	$\Omega_c$	3094	3279	3050
$\overline{\mathbf{15}}_{3/2}^c(J=1)$	$B_c$	2750	3020	2754
$\overline{\mathbf{15}}_{3/2}^c(J=1)$	$\Sigma_c$	2887	3121	2877
$\overline{\mathbf{15}}_{3/2}^c(J=1)$	$\Lambda_c$	2894	3143	2875
$\overline{\mathbf{15}}_{3/2}^c(J=1)$	$\Xi_c$	3028	3245	2997
$\overline{\mathbf{15}}_{3/2}^c(J=1)$	$\Xi_c^{3/2}$	3017	3213	3000
$\overline{\mathbf{15}}_{3/2}^c(J=1)$	$\Omega_c$	3162	3347	3119

shown previously, the baryon antitriplet and sextet naturally arise as the representations of the rotational excitations with  $Y' = 2/3$ . The next allowed representation is the baryon antidecapentaplet ( $\overline{\mathbf{15}}$ ) with  $Y' = 2/3$ . The valence quark content of the baryon decapentaplet is  $Qqqq\bar{q}$ , where  $Q$  and  $q$  denote the heavy and light quarks respectively.  $\bar{q}$  stands for the anti-light quark. So, the members of the  $\overline{\mathbf{15}}$ -plet are the pentaquark baryons including one heavy quark. Coupling the soliton spins 0 and 1 to the heavy-quark spin 1/2, we find three different spin representations in the baryon antidecapentaplet with 1/2 and (1/2, 3/2). As shown in Eqs. (39) and (40), the values of  $M_{B, \overline{\mathbf{15}}_1^c, J=0}^Q$  are larger than those of  $M_{B, \overline{\mathbf{15}}_1^c, J=1}^Q$  and  $M_{B, \overline{\mathbf{15}}_{3/2}^c, J=1}^Q$ .

Table VII lists the numerical results of the masses of the charmed baryon antidecapentaplet. As mentioned previously, the results of  $M_{B, \overline{\mathbf{15}}_1^c, J=0}^c$  are larger than the corresponding ones of  $M_{B, \overline{\mathbf{15}}_1^c, J=1}^Q$  and  $M_{B, \overline{\mathbf{15}}_{3/2}^c, J=1}^Q$ . Though there are no experimental data on them, it is of great interest to consider the masses of  $\Omega_c$ 's, in particular, when the soliton spin is  $J = 1$ . In Ref. [15],  $\Omega_c(3050)$  and  $\Omega_c(3119)$  were interpreted as possible pentaquark states that belong to the  $\overline{\mathbf{15}}$ -plet. In the present work, we obtain  $M_{\Omega_c, 1/2} = 3094$  MeV and  $M_{\Omega_c, 3/2} = 3162$ , which are somewhat larger than those of Ref. [15]. In Table VIII, we list the results of the masses of the bottom baryon antidecapentaplet. In general, the present results are again larger than those predicted by Ref. [15].

- 
- [1] E. Witten, Nucl. Phys. B **160**, 57 (1979).
  - [2] E. Witten, Nucl. Phys. B **223**, 422 (1983).
  - [3] E. Witten, Nucl. Phys. B **223**, 433 (1983).
  - [4] D. Diakonov, V. Y. Petrov and P. V. Pobylitsa, Nucl. Phys. B **306** (1988) 809.
  - [5] C. V. Christov, A. Blotz, H.-Ch. Kim, P. Pobylitsa, T. Watabe, T. Meissner, E. Ruiz Arriola and K. Goeke, Prog. Part. Nucl. Phys. **37**, 91 (1996).
  - [6] D. Diakonov, In \*Peniscola 1997, Advanced school on non-perturbative quantum field physics\* 1-55 [hep-ph/9802298].
  - [7] A. Blotz, D. Diakonov, K. Goeke, N. W. Park, V. Petrov and P. V. Pobylitsa, Nucl. Phys. A **555**, 765 (1993).
  - [8] D. Diakonov, arXiv:1003.2157 [hep-ph].

TABLE VIII. Results of the masses of the charmed baryon antidecaplet in units of MeV in comparison with those of Ref. [15]. The fourth column lists the results obtained by using the  $N_c$  pion mean fields [10].

$\mathcal{R}_{J'}^Q$	$B_Q$	This work	[10]*	[15]
$\overline{\mathbf{15}}_{1/2}^b(J=0)$	$B_b$	6239	6511	-
$\overline{\mathbf{15}}_{1/2}^b(J=0)$	$\Sigma_b$	6402	6674	-
$\overline{\mathbf{15}}_{1/2}^b(J=0)$	$\Lambda_b$	6366	6638	-
$\overline{\mathbf{15}}_{1/2}^b(J=0)$	$\Xi_b$	6511	6782	-
$\overline{\mathbf{15}}_{1/2}^b(J=0)$	$\Xi_b^{3/2}$	6564	6836	-
$\overline{\mathbf{15}}_{1/2}^b(J=0)$	$\Omega_b$	6655	6927	-
$\overline{\mathbf{15}}_{1/2}^b(J=1)$	$B_b$	6043	6261	6044
$\overline{\mathbf{15}}_{1/2}^b(J=1)$	$\Sigma_b$	6181	6399	6167
$\overline{\mathbf{15}}_{1/2}^b(J=1)$	$\Lambda_b$	6188	6406	6165
$\overline{\mathbf{15}}_{1/2}^b(J=1)$	$\Xi_b$	6322	6540	6287
$\overline{\mathbf{15}}_{1/2}^b(J=1)$	$\Xi_b^{3/2}$	6311	6529	6290
$\overline{\mathbf{15}}_{1/2}^b(J=1)$	$\Omega_b$	6456	6674	6409
$\overline{\mathbf{15}}_{3/2}^b(J=1)$	$B_b$	6064	6281	6065
$\overline{\mathbf{15}}_{3/2}^b(J=1)$	$\Sigma_b$	6201	6419	6188
$\overline{\mathbf{15}}_{3/2}^b(J=1)$	$\Lambda_b$	6208	6426	6186
$\overline{\mathbf{15}}_{3/2}^b(J=1)$	$\Xi_b$	6342	6560	6308
$\overline{\mathbf{15}}_{3/2}^b(J=1)$	$\Xi_b^{3/2}$	6331	6549	6311
$\overline{\mathbf{15}}_{3/2}^b(J=1)$	$\Omega_b$	6476	6694	6430

- [9] Gh.-S. Yang, H.-Ch. Kim, M. V. Polyakov, and M. Praszalowicz, Phys. Rev. D **94**, 071502 (2016).  
[10] J. Y. Kim, H.-Ch. Kim and G. S. Yang, Phys. Rev. D **98**, no. 5, 054004 (2018).  
[11] G. S. Yang and H.-Ch. Kim, Phys. Lett. B **781**, 601 (2018).  
[12] J. Y. Kim and H.-Ch. Kim, Phys. Rev. D **97**, 114009 (2018).  
[13] R. Aaij *et al.* [LHCb Collaboration], Phys. Rev. Lett. **118**, 182001 (2017).  
[14] J. Yelton *et al.* [Belle Collaboration], Phys. Rev. Lett. **121** 052003 (2018).  
[15] H.-Ch. Kim, M. V. Polyakov, and M. Praszalowicz, Phys. Rev. D **96**, 014009 (2017); **96**, 039902(E) (2017).  
[16] H.-Ch. Kim, M. V. Polyakov, M. Praszalowicz and G. S. Yang, Phys. Rev. D **96**, 094021 (2017) Erratum: [Phys. Rev. D **97**, 039901 (2018)].  
[17] H.-Ch. Kim, J. Korean Phys. Soc. **73**, no. 2, 165 (2018) [arXiv:1804.04393 [hep-ph]].  
[18] M. V. Polyakov and P. Schweitzer, Int. J. Mod. Phys. A **33**, 1830025 (2018).  
[19] J.-Y. Kim, H.-D. Son, M. V. Polyakov, and H.-Ch. Kim, in preparation (2020).  
[20] M. Tanabashi *et al.* [Particle Data Group], Phys. Rev. D **98**, no. 3, 030001 (2018).  
[21] A. Momen, J. Schechter and A. Subbaraman, Phys. Rev. D **49**, 5970 (1994).  
[22] I. Zahed and G. E. Brown, Phys. Rept. **142**, 1 (1986).